Cite as: Martinez JA, Taljanovic MS, Witte RS, Nuncio Zuniga AA, Wertheim BC, Kwoh CK, Goldstein BA, Roe DJ, Chalasani P: Shear wave elastography detects novel imaging biomarkers of aromatase inhibitor – induced joint pain: a pilot study. J Ultrason 2021; 21: e1–e6. doi: 10.15557/JoU.2021.0001.

Submitted: 28.07.2020
Accepted: 15.11.2020
Published: 08.03.2021

Shear wave elastography detects novel imaging biomarkers of aromatase inhibitor–induced joint pain: a pilot study

Jessica A. Martinez[1,2], Mihra S. Taljanovic[3,4], Russell S. Witte[1,5], Andres A. Nuncio Zuniga[5], Betsy C. Wertheim[1], C. Kent Kwoh[3,6,7], Brian A. Goldstein[5], Denise J. Roe[1,8], Pavani Chalasani[1,7]

[1] *The University of Arizona Cancer Center, Tucson, AZ, USA*
[2] *Department of Nutritional Sciences, University of Arizona, Tucson, AZ, USA*
[3] *Department of Medical Imaging, University of Arizona, Tucson, AZ, USA*
[4] *Department of Orthopaedic Surgery, University of Arizona, Tucson, AZ, USA*
[5] *Department of Biomedical Engineering, University of Arizona, Tucson, AZ, USA*
[6] *The University of Arizona Arthritis Center, Tucson, AZ, USA*
[7] *Department of Medicine, University of Arizona, Tucson, AZ, USA*
[8] *Department of Epidemiology and Biostatistics, University of Arizona, Tucson, AZ, USA*

Correspondence: Jessica A. Martinez, 1515 N Campbell Ave, Tucson, AZ; tel.: (520) 626 6326, fax: (520) 626 5348, e-mail: jam1@email.arizona.edu

DOI: 10.15557/JoU.2021.0001

Keywords
aromatase inhibitors, breast cancer, arthralgia, Doppler ultrasound, shear wave elastography

Abstract

Aim: To determine whether differences in joint and tendon stiffness as measured by ultrasound shear wave elastography are present in breast cancer patients with aromatase inhibitor-associated arthralgias compared to age-comparable healthy control women. **Methods:** Postmenopausal women with stage I–III breast cancer who were taking adjuvant aromatase inhibitors and complained of joint pain were enrolled (n = 6). Postmenopausal women with no history of breast cancer, hormone treatment, or joint pain served as controls (n = 7). All subjects had bilateral hands and wrists evaluated by gray-scale and power Doppler ultrasound, and shear wave elastography ultrasound. **Results:** Patients with AI-associated arthralgias had significantly stiffer tendons than controls in the 1st extensor compartment (long axis; p = 0.001), 4th extensor compartment (long axis; p = 0.014), 3rd metacarpophalangeal joint (p = 0.002), the pooled values of the extensor compartments, both long (p = 0.044) and short axes (p = 0.035), and the pooled values for the metacarpophalangeal joints (p = 0.002). On ultrasound, the patients (but not controls) presented with hyperemia and increased tenosynovial fluid in the flexor and extensor tendon sheaths, and the median nerves were symptomatic and bifid; however, these differences were not statistically significant. **Conclusions:** This is the first study to identify increased tendon stiffness as a putative physiological characteristic of aromatase inhibitor–associated arthralgias. Future studies should determine whether increased tendon stiffness is a risk factor for the development of aromatase inhibitor–associated arthralgias, or a result of aromatase inhibitor treatment.

Introduction

Aromatase inhibitors (AIs) have become first-line standard adjuvant endocrine therapy for postmenopausal women with hormone receptor positive (HR+) breast cancer. Although outcomes have improved compared to tamoxifen[1], AI therapy has been associated with significant, activity-limiting musculoskeletal symptoms including arthralgia, myalgia, and joint stiffness, collectively called AI-associated arthralgias (AIA)[2,3]. Among the most commonly reported side effects experienced by patients on AI therapy are musculoskeletal-related symptoms including joint pain and joint stiffness, with up to 50% of women reporting joint-related symptoms[4,5].

Musculoskeletal-related symptoms manifest early after initiation of AI therapy and worsen for up to 1 year[6,7]. A number of studies have revealed high discontinuation of AIs (31–73%) and low adherence (41–72%) after 5 years[8]. A large observational study (n = 12,391) showed that 32–50% of women were considered nonadherent to the AI anastrozole (defined as <80% of drug coverage days) after 3 years[9]. Given that low adherence to AIs has been directly related to increased risk of breast cancer-specific mortality[10], it is key to identify those at risk of developing AIA. However, there are no biomarkers to indicate targetable pathways of AIA. Current standard clinical practice is to administer nonsteroidal anti-inflammatory drugs (NSAIDs) to manage symptoms or to switch AIs[11].

Imaging studies using ultrasound (US) and magnetic resonance imaging (MRI) of hands/wrists to determine physiological changes and biomarkers associated with AIA show ambiguous results. While some demonstrate increased tendon thickness and fluid among women on AIs[12,13], other studies have shown no such difference[14,15]. Morales *et al*. showed that the loss of grip strength was correlated with worsening of abnormal tenosynovial findings on MRI[16] and with development of AIA symptoms in 6-month[17] and 2-year[18] prospective studies. However, there are no biomarkers to identify those at risk of developing AIA. Identifying women at risk for developing AIA is critical in order to study interventions to prevent AIA, improve AI adherence, and prevent breast cancer recurrence and death.

Shear wave elastography (SWE) is a novel US technique for characterizing tissue structures with shear acoustic waves of a focused ultrasonic beam[19] to acquire a measure of tendon stiffness. We conducted a pilot study to evaluate tendon features of the hands and wrists using SWE US imaging in postmenopausal women on AIs with AIA versus healthy controls. Since tendinopathic tendons have decreased SW velocities (i.e. are softer) compared to healthy normal tendons[20], we hypothesized that women with AIA would have softer tendons than controls. To our knowledge, this is the first study to utilize SWE in the context of AIA.

Material and methods

Participants

This study was approved by the University of Arizona Institutional Review Board, and all participants provided written informed consent (IRB# 1404308335). The enrolled subjects were stage I–II breast cancer patients that were treated at the University of Arizona Cancer Center (UACC) with a non-steroidal AI for their adjuvant therapy and complained of joint pain (n = 6). None of the patients had joint pain prior to starting AI treatment. Healthy volunteers with no history of breast cancer or any type of joint pain were recruited from faculty at UACC (n = 7). None of the volunteers were taking hormone replacement of any kind. All participants were postmenopausal women.

Gray-Scale and power Doppler, and shear wave elastography (SWE) ultrasound (US) imaging

Real-time gray-scale and power Doppler US examination of bilateral wrists and hands were performed on a General Electric Logiq E9 machine using the 18–8 MHz linear hockey stick transducer per our routine inflammatory arthritis protocol. Dorsal and volar aspects of the 2nd, 3rd, and 5th metacarpophalangeal (MCP) joints were examined in their long and short axes. Additionally, all six extensor compartment tendons and tendon sheaths, as well as flexor tendons in the carpal tunnel and the median nerve, were examined in their long and short axes. US examination of the flexor and/or extensor tendons was performed along the digits/fingers.

During US examination, patients were seated with their hands resting on a small table placed between the examiner and the patient. All joints were examined for the presence of cortical erosions on gray-scale US. All joints, tendons, and tendon sheaths were evaluated for the presence of increased synovial fluid complex on gray-scale evaluation and for the presence of hyperemia on power Doppler evaluation. We also examined the median nerve for hyperemia, and patients were asked whether they experienced pain, numbness, tingling, or muscle weakness in the palm, thumb, index, middle or little fingers ("symptomatic" findings). In addition, the presence or absence of soft tissue edema was recorded. Results for each finding were scored as present (1) or absent (0).

SWE US examinations of the bilateral wrists and hands were then performed on a Siemens S3000 unit (Siemens Medical Systems) with a high-resolution 9-MHz linear transducer. The tissue elasticity (degree of stiffness) was displayed on color bar elastogram on the US screen and expressed as SW velocities in m/s. A copious amount of ultrasound gel was used to accommodate the depth. The radial aspect of the 2nd and 3rd MCP joints and the ulnar aspect of the 5th MCP joints were examined in their long axes.

At the dorsal aspect of each wrist and hand, SWE of all six extensor compartment tendons was performed in the long and short axes. At the volar aspect of each wrist, SWE of the flexor tendons and the median nerves was performed, centered in the carpal tunnel region. SWE of the flexor and extensor tendons was performed along the digits/fingers.

Shear wave elastography (SWE) scoring

Ultrasound B-mode DICOM images taken by the Siemens ACUSON S3000 were examined by a trained radiologist to determine regions of interest (ROIs) containing anatomical structures of interest: the 1st, 2nd, 4th, and 6th extensor compartments; the 2nd, 3rd, and 5th MCP joints; the median nerve; and the volar flexors adjacent to the median nerve. The B-mode images were co-registered with SW velocity color maps. Depending on the size, each ROI contained 6,000–20,000 pixels; the average SW velocity of all the

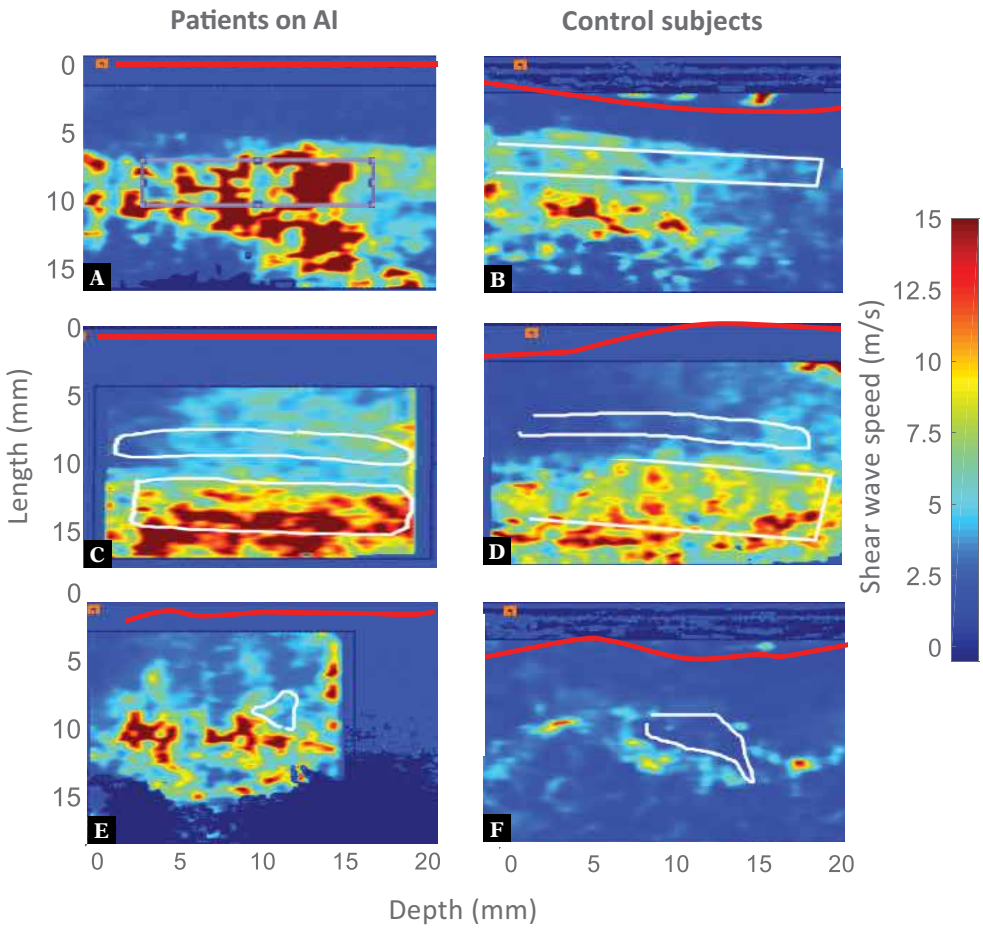

Fig. 1. *Example SWE images comparing AI versus control. Red line indicates location of skin surface.* **A.** *Extensor compartment 1 from an AI patient.* **B.** *Extensor compartment 1 from a control subject.* **C.** *Volar flexor tendon and median nerve from an AI patient.* **D.** *Volar flexor tendon and median nerve from a control subject.* **E.** *Metacarpophalangeal (MCP) joint from an AI patient (short axis).* **F.** *MCP joint from a control (short axis)*

pixels contained within each ROI was calculated using color map values and tabulated. Each compartment contains multiple tendons (except the 6th). When compartments are imaged along the short axis, multiple tendons are captured within an ROI; therefore, the reported SWE velocities represent an average of multiple tendons in a given compartment. For the longitudinal collection of the compartments, one representative tendon was chosen by the radiologist for scoring.

Tab. 1. *Breast cancer patient demographics (n = 6)*

Characteristic	*n* (%)
Age at diagnosis: *mean (range)*	58 (43–69) y
Surgery • Lumpectomy • Mastectomy	 4 (67%) 2 (33%)
Adjuvant radiation therapy	4 (67%)
Adjuvant chemotherapy	2 (33%)
Stage • I • II	 4 (67%) 2 (33%)
Duration on AI:[1] *mean (range)*	13.2 (4–20) months
[1] Duration on an aromatase inhibitor before ultrasound imaging	

Statistical methods

Ages of the healthy controls and AI patients were compared using a two-sample independent t-test. Fisher's exact test was used to assess between-group differences in characteristics determined by US imaging. Between-group differences in SW velocity was determined using linear mixed models, initially clustered on participant and then further adjusted for area of the ROI. A p-value <0.05 was considered significant.

Results

Participant characteristics

The mean age of healthy controls was 59.3 years (range 54–72 y) which was not different from the mean age of breast cancer patients on AI at the time of imaging (60.0 y, range 45–70 y; t-test $p = 0.88$). All 7 healthy controls were non-Hispanic white, whereas 4 of the breast cancer patients were non-Hispanic white and 2 were Hispanic. For the breast cancer patients, the mean duration of AI at the time of imaging was 13.2 months (range 4–20 months) (Tab. 1). Four of the patients

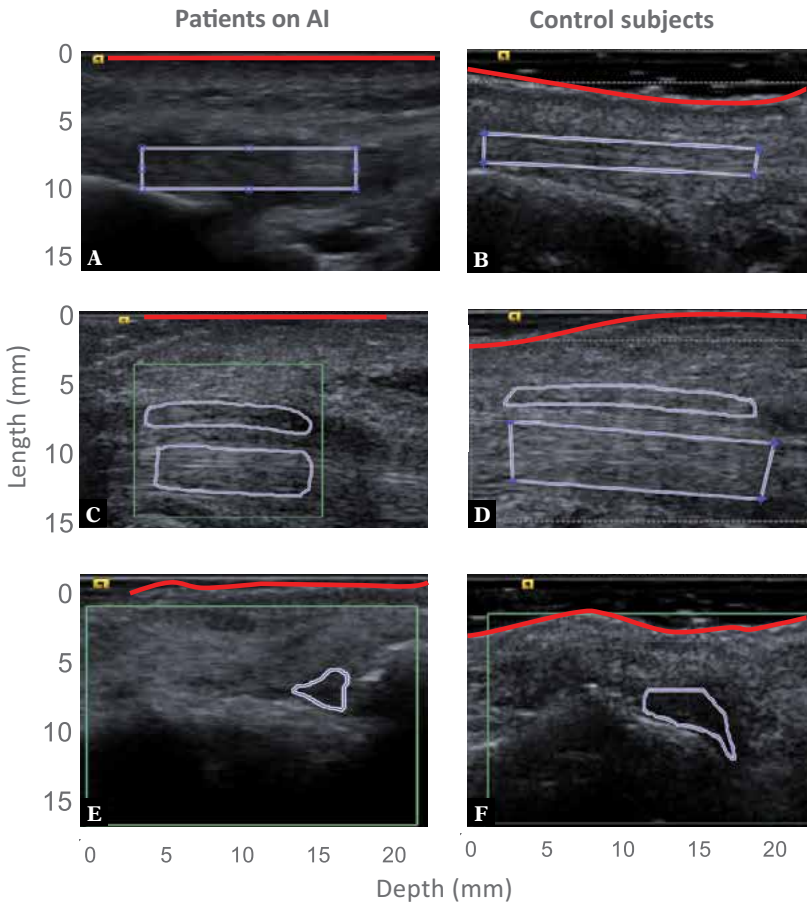

Fig. 2. *Example gray-scale images comparing AI and control. Red line indicates location of skin surface.* **A.** *Extensor compartment 1 from an AI patient.* **B.** *Extensor compartment 1 from a control subject.* **C.** *Volar flexor tendon and median nerve from an AI patient.* **D.** *Volar flexor tendon and median nerve from a control subject.* **E.** *Metacarpophalangeal (MCP) joint from an AI patient (short axis).* **F.** *MCP joint from a control (short axis)*

had lumpectomy, radiation therapy and were stage I; two had a mastectomy, received chemotherapy and were stage II.

Gray-scale and power Doppler ultrasound imaging

Table 2 shows presence or absence of abnormal imaging findings at the MCP joints, wrists, flexor and extensor tendons, and the median nerve using gray-scale and power Doppler US. There were no significant differences in increased joint fluid, hyperemia, or cortical irregularity between controls and the AI group. In the median nerve, there were no significant differences in the presence of hyperemia, symptomatic findings, or bifid anatomy. Taken together, 7 of 7 controls had all negative median nerve findings (no hyperemia, not symptomatic, not bifid) compared to 2 of 6 in AI group; $p = 0.020$.

Shear wave elastography (SWE)

Figure 1 illustrates representative SW US images from the 1st extensor compartment (A, B), the median nerve (C, D), the volar flexor (C, D), and the MCP joint (E, F) from patients on AI (left panels) and control subjects (right panels). The SW velocity is represented by a color scale

Tab. 2. *Results from grayscale and power Doppler ultrasound imaging of the hands and wrists*

Clinical site and finding	Control	AI	*p*-value[a]
MCP joints			
• Increased joint fluid	0/7 (0%)	2/6 (33%)	0.19
• Hyperemia	0/7 (0%)	2/6 (33%)	0.19
• Cortical irregularity	0/7 (0%)	0/6 (0%)	n/a
• All above negative	7/7 (100%)	4/6 (67%)	0.19
Wrists			
• Increased joint fluid	1/7 (14%)	3/6 (50%)	0.27
• Hyperemia	0/7 (0%)	1/6 (17%)	0.46
• Cortical irregularity	0/7 (0%)	1/6 (17%)	0.46
• All above negative	6/7 (86%)	3/6 (50%)	0.27
Flexor & extensor tendons			
• Increased Tenosynovial fluid	0/7 (0%)	3/6 (50%)	0.07
• Hyperemia	0/7 (0%)	3/6 (50%)	0.07
• All above negative	7/7 (100%)	3/6 (50%)	0.07
Median nerve			
• Hyperemia	0/7 (0%)	1/6 (17%)	0.46
• Symptomatic	0/7 (0%)	3/6 (50%)	0.07
• Bifid	0/7 (0%)	3/6 (50%)	0.07
• All above negative	7/7 (100%)	2/6 (33%)	0.02
MCP – metacarpophalangeal			
[a] Fisher's Exact Test			

Tab. 3. *Velocity determined by shear wave elastography (SWE)*[a]

Image location	AI		CL		Model 1[b]		Model 2[c]	
	n	median (IQR)	*n*	median (IQR)	beta	*p*	beta	*p*
1st Extensor compartment (long axis)[d,e]	5	8.52 (7.45–10.26)	5	5.70 (4.84–7.14)	3.57	0.001	3.40	0.003
1st Extensor compartment (short axis)[f,e]	4	5.51 (5.42–7.89)	4	4.37 (3.71–5.34)	2.28	0.061	2.79	0.036
2nd Extensor compartment (short axis)[e]	4	5.36 (4.69–6.67)	4	4.99 (3.94–6.09)	0.53	0.586	0.69	0.445
4th Extensor compartment (long axis)[e]	5	7.12 (6.78–7.94)	7	5.82 (5.14–7.76)	1.42	0.014	1.20	0.039
6th Extensor compartment (long axis)	5	9.53 (7.78–12.95)	6	9.32 (8.09–11.5)	1.15	0.441	1.12	0.456
2nd MCP (radial dorsal image)[g]	6	5.86 (4.78–6.39)	5	4.78 (4.39–5.00)	0.84	0.220	0.75	0.276
3rd MCP (radial dorsal image)	6	6.37 (5.09–8.31)	5	4.60 (3.81–4.61)	2.79	0.002	1.89	0.008
5th MCP (ulnar dorsal image)[h]	5	5.22 (4.68–6.55)	5	4.61 (4.28–4.80)	1.12	0.093	1.16	0.083
Median nerve	6	4.60 (4.29–4.88)	7	4.89 (3.46–6.20)	–0.68	0.549	–0.80	0.183
Volar flexors (long axis)	6	8.31 (6.47–8.93)	7	8.76 (7.41–9.82)	–0.07	0.956	–0.12	0.927
Extensor compartments pooled (long axis)[i]	5	8.83 (7.57–10.26)	7	7.44 (5.82–11.6)	1.62	0.044	1.74	0.040
Extensor compartments pooled (short axis)[j]	4	5.73 (5.26–5.95)	4	5.13 (4.11–5.44)	1.40	0.035	1.40	0.032
Synovial fluid complexes of the MCP joints pooled[k]	6	5.46 (5.09–6.34)	5	4.80 (4.28–4.94)	1.73	0.002	1.30	0.011
Volar flexors pooled (long + short axis)[l]	6	8.76 (7.41–9.82)	7	8.76 (7.41–9.82)	–0.09	0.941	0.07	0.952

[a] Not all anatomical images were available for all participants. Anatomical locations were analyzed separately if they were captured in at least 4 AI patients and 4 controls. Images were analyzed from the left, right, or both hands if available.
[b] Linear mixed model of velocity, clustered on person; n is the number of people, not the number of hands
[c] Linear mixed model of velocity, adjusted for area, clustered on person
[d] Long axis images were acquired along the longitudinal section of the anatomical site
[e] SWE velocities were averaged for all tendons within each compartment
[f] Short axis images were acquired along the cross-section of the anatomical site
[g] Radial images were acquired on the same side as the radius
[h] Ulnar images were acquired on the same side as the ulna
[i] Includes 1st, 2nd, 4th, and 6th extensor compartments – all longitudinal axis images
[j] Includes 1st, 2nd, 4th, and 6th extensor compartments – all cross-sectional images
[k] Includes 2nd, 3rd, and 5th MCP radial images + 2nd, 3rd, and 5th MCP ulnar images
[l] Includes both longitudinal and cross-sectional images of the volar flexors

such that blue is the slowest (0 m/s; least stiff) and red is the fastest (15 m/s; most stiff). Faster SW velocities can be visualized for AI tendons versus control. Figure 2 illustrates the grayscale images of the locations imaged in Fig. 1 in order to assist visualization of the anatomical sites.

Table 3 presents the velocity determined by SWE, where a faster velocity indicates stiffer tendons. The 1st extensor compartment tendons and tendon sheaths were significantly stiffer in postmenopausal women on AI than controls in both the long ($p = 0.003$) and short axes ($p = 0.036$). The 4th extensor compartment tendons and tendon sheaths were significantly stiffer among AI women than controls ($p = 0.039$). Pooled extensor compartments were stiffer in AI patients than controls along both the longitudinal ($p = 0.040$) and short ($p = 0.032$) axes. The 3rd MCP was significantly stiffer in AI than controls ($p = 0.027$) as well as of all MCP joints combined ($p = 0.008$). There was no difference between AI and control in the stiffness of the 2nd or 6th extensor compartments, the 2nd or 5th MCP joints, the median nerve, or the volar flexors.

Discussion

In light of recent evidence supporting extended adjuvant AI treatment to 10 years, the need to understand the pathophysiology of AIA is even more important in order to improve adherence over a longer duration of treatment[21]. Our pilot data suggest that AIA is partially characterized by the presence of increased tendon stiffness compared to age-comparable, healthy women. To our knowledge, this is the first clinical study to evaluate tendon stiffness in breast cancer patients on AI utilizing SWE.

SWE is a robust, noninvasive technique to quantify tissue stiffness and identify tendon pathology at different locations, and it has been shown to significantly improve the diagnostic accuracy of traditional tendon US examination[20]. Multiple studies suggest that tendinopathic tendons (including rheumatoid arthritis) have decreased SW velocities compared to healthy normal tendons[20,22]. However, our results suggest that women with AIA have stiffer tendons and increased SW velocities than age-comparable healthy women. These differences could be related to the depletion of estrogen with AI treatment. One study reported that during the follicular phase of the menstrual cycle, muscles were significantly stiffer (evaluated by SWE) than during ovulation[23]. This greater muscle stiffness during the follicular phase was associated with significantly lower estradiol than during ovulation. To our knowledge, however, no studies have evaluated tendon or joint stiffness in relationship to estradiol levels. In addition, it is also possible that the stiffer tendons and joints observed in the AIA group in the current pilot study are due to factors that were not controlled, such as occupation, BMI, or diet. Nevertheless, given that AI treatment has also been shown to increase the risk of rheumatoid arthritis[24], this study provides preliminary evidence supporting SWE as a valuable, objective modality to help understand the physiology of AIA and to distinguish it from other causes of joint pain, such as rheumatoid arthritis or osteoarthritis. Importantly, SWE was able to detect differences in tendon stiffness between AI patients and controls, whereas routine US examination was not.

We were limited by a very small sample size, cross-sectional design, and lack of asymptomatic women taking AI. Therefore, it is unknown if our observation that patients with

AIA have stiffer tendons is a result of AI treatment alone, or if stiffer tendons are specific to those at risk for arthralgias. Furthermore, it is possible that selection bias led to differences between groups (e.g. socioeconomic status, occupation), which were not evaluated in this study and could be responsible for the observed differences. It is also possible that our observed differences are due to chance given our very small samples size. All *p*-values should be interpreted with caution, as this pilot study was not adequately powered. A strength of our study is that we were able to use an ROI around each anatomical structure, averaging the SWE velocities of 6,000–20,000 pixels for each structure; however, each structural image was captured only once. The radiologist was as consistent as possible with regard to tendon angle, pressure, and overall technique; however, any differences in these factors can affect the SW velocities. We were also limited in the number of anatomic sites that we were able to evaluate; however, the results presented here support justification for a prospective study with a more complete evaluation of the hands and wrists, as well as other commonly affected sites in AIA, such as the knees and hips.

Conclusions

To our knowledge, we are the first to identify increased tendon stiffness as an imaging biomarker of AIA. Despite its limitations, this pilot study provides the first reported evidence supporting future prospective studies to determine whether tendon stiffness is a risk factor for the development of AIA, a result of AI treatment, or both.

Acknowledgments

We would like to thank ultrasound technologist Amanda Hadden for her work in obtaining the ultrasound images.

Conflict of interest

Authors do not report any financial or personal connections with other persons or organizations, which might negatively affect the contents of this publication and/or claim authorship rights to this publication.

References

1. Bentzon N, During M, Rasmussen BB, Mouridsen H, Kroman N: Prognostic effect of estrogen receptor status across age in primary breast cancer. Int J Cancer 2008; 122: 1089–1094.
2. Park SH, Knobf MT, Sutton KM: Etiology, assessment, and management of aromatase inhibitor-related musculoskeletal symptoms. Clin J Oncol Nurs 2012; 16: 260–266.
3. Henry NL, Giles JT, Ang D, Mohan M, Dadabhoy D, Robarge J *et al.*: Prospective characterization of musculoskeletal symptoms in early stage breast cancer patients treated with aromatase inhibitors. Breast Cancer Res Treat 2008; 111: 365–372.
4. Crew KD, Greenlee H, Capodice J, Raptis G, Brafman L, Fuentes D *et al.*: Prevalence of joint symptoms in postmenopausal women taking aromatase inhibitors for early-stage breast cancer. J Clin Oncol 2007; 25: 3877–3883.
5. Zivian MT, Salgado B: Side Effects Revisited: Women's Experiences with Aromatase Inhibitors. Breast Cancer Action, San Francisco 2008.
6. Howell A, Cuzick J, Baum M, Buzdar A, Dowsett M, Forbes JF *et al.*: Results of the ATAC (Arimidex, Tamoxifen, Alone or in Combination) trial after completion of 5 years' adjuvant treatment for breast cancer. Lancet 2005; 365: 60–62.
7. Castel LD, Hartmann KE, Mayer IA, Saville BR, Alvarez J, Boomershine CS *et al.*: Time course of arthralgia among women initiating aromatase inhibitor therapy and a postmenopausal comparison group in a prospective cohort. Cancer 2013; 119: 2375–2382.
8. Murphy CC, Bartholomew LK, Carpentier MY, Bluethmann SM, Vernon SW: Adherence to adjuvant hormonal therapy among breast cancer survivors in clinical practice: a systematic review. Breast Cancer Res Treat 2012; 134: 459–478.
9. Partridge AH, LaFountain A, Mayer E, Taylor BS, Winer E, Asnis-Alibozek A: Adherence to initial adjuvant anastrozole therapy among women with early-stage breast cancer. J Clin Oncol 2008; 26: 556–562.
10. Makubate B, Donnan PT, Dewar JA, Thompson AM, McCowan C: Cohort study of adherence to adjuvant endocrine therapy, breast cancer recurrence and mortality. Br J Cancer 2013; 108: 1515–1524.
11. Briot K, Tubiana-Hulin M, Bastit L, Kloos I, Roux C: Effect of a switch of aromatase inhibitors on musculoskeletal symptoms in postmenopausal women with hormone-receptor-positive breast cancer: the ATOLL (articular tolerance of letrozole) study. Breast Cancer Res Treat 2010; 120: 127–134.
12. Dizdar O, Ozcakar L, Malas FU, Harputluoglu H, Bulut N, Aksoy S *et al.*: Sonographic and electrodiagnostic evaluations in patients with aromatase inhibitor-related arthralgia. J Clin Oncol 2009; 27: 4955–4960.
13. Morales L, Pans S, Paridaens R, Westhovens R, Timmerman D, Verhaeghe J *et al.*: Debilitating musculoskeletal pain and stiffness with letrozole and exemestane: associated tenosynovial changes on magnetic resonance imaging. Breast Cancer Res Treat 2007; 104: 87–91.
14. Shanmugam VK, McCloskey J, Elston B, Allison SJ, Eng-Wong J: The CIRAS study: a case control study to define the clinical, immunologic, and radiographic features of aromatase inhibitor-induced musculoskeletal symptoms. Breast Cancer Res Treat 2012; 131: 699–708.
15. Henry NL, Jacobson JA, Banerjee M, Hayden J, Smerage JB, Van Poznak C *et al.*: A prospective study of aromatase inhibitor-associated musculoskeletal symptoms and abnormalities on serial high-resolution wrist ultrasonography. Cancer 2010; 116: 4360–4367.
16. Morales L, Pans S, Verschueren K, Van Calster B, Paridaens R, Westhovens R *et al.*: Prospective study to assess short-term intra-articular and tenosynovial changes in the aromatase inhibitor-associated arthralgia syndrome. J Clin Oncol 2008; 26: 3147–3152.
17. Singer O, Cigler T, Moore AB, Levine AB, Hentel K, Belfi L *et al.*: Defining the aromatase inhibitor musculoskeletal syndrome: a prospective study. Arthritis Care Res (Hoboken) 2012; 64: 1910–1918.
18. Lintermans A, Laenen A, Van Calster B, Van Hoydonck M, Pans S, Verhaeghe J *et al.*: Prospective study to assess fluid accumulation and tenosynovial changes in the aromatase inhibitor-induced musculoskeletal syndrome: 2-year follow-up data. Ann Oncol 2013; 24: 350–355.
19. Sarvazyan AP, Rudenko OV, Swanson SD, Fowlkes JB, Emelianov SY: Shear wave elasticity imaging: a new ultrasonic technology of medical diagnostics. Ultrasound Med Biol 1998; 24: 1419–1435.
20. Taljanovic MS, Gimber LH, Becker GW, Latt LD, Klauser AS, Melville DM *et al.*: Shear-wave elastography: basic physics and musculoskeletal applications. Radiographics 2017; 37: 855–870.
21. Burstein HJ, Lacchetti C, Anderson H, Buchholz TA, Davidson NE, Gelmon KA *et al.*: Adjuvant endocrine therapy for women with hormone receptor-positive breast cancer: ASCO clinical practice guideline focused update. J Clin Oncol 2019; 37: 423–438.
22. Dirrichs T, Quack V, Gatz M, Tingart M, Kuhl CK, Schrading S: Shear wave elastography (SWE) for the evaluation of patients with tendinopathies. Acad Radiol 2016; 23: 1204–1213.
23. Ham S, Kim S, Choi H, Lee Y, Lee H: Greater muscle stiffness during contraction at menstruation as measured by shear-wave elastography. Tohoku J Exp Med 2020; 250: 207–213.
24. Caprioli M, Carrara G, Sakellariou G, Silvagni E, Scire CA: Influence of aromatase inhibitors therapy on the occurrence of rheumatoid arthritis in women with breast cancer: results from a large population-based study of the Italian Society for Rheumatology. RMD Open 2017; 3: e000523.